Effect of discrete coherent structures on nonlinear interactions in the scrape-off-layer

D. A. D'Ippolito and J. R. Myra

Lodestar Research Corporation, 2400 Central Avenue, Boulder, Colorado 80301

May, 2008

Effect of discrete coherent structures on nonlinear interactions in the scrape-off-layer *

D. A. D'Ippolito[†] and J. R. Myra

Lodestar Research Corporation,
2400 Central Avenue, Boulder, Colorado 80301

Abstract

The effect of discrete plasma transport by coherent structures on nonlinear interactions in the scrape-off-layer (SOL) is illustrated by a simple model problem. A one-dimensional ballistic model is studied in which a periodic train of plasma blobs creates a series of discrete pulses of neutral atoms by sputtering of a high-Z wall. Collisions between the neutral pulses and blobs lead to ionization of the high-Z atoms, convective transport back to the wall, and subsequent self-sputtering. An analytic condition for high-Z impurity avalanche is calculated and evaluated taking into account the effect of the temperature nonlinearity of the ionization rate. It is shown that the discreteness of the blob particle and energy transport leads to quite different results than a continuum model with the same average density and temperature. Similar effects are expected in fully intermittent transport due to turbulence or edge localized modes (ELMs) in the SOL of tokamaks. The model calculations also illustrate a potentially important interaction between high-power radiofrequency antennas and high-Z walls.

PACS numbers: 52.35.Ra, 52.25.Vy, 52.40.Hf, 52.55.Fa

†email: **dippolito@lodestar.com**

A great deal of theoretical and experimental work has shown that convective transport by turbulent coherent structures [e.g. blobs or Edge Localized Modes (ELMs)] dominates the particle and energy transport in the far scrape-off-layer (SOL) of tokamaks. (See Refs. 1 and 2 for recent reviews.) As a result, the electron density n_e and temperature T_e in the far SOL are spatially and temporally discrete and intermittent, and interactions that are nonlinear in these field variables are not well described in the continuum or time-averaged limit.[2] This problem can be expressed as

$$\langle f(Q) \rangle \neq f(\langle Q \rangle) \ , \tag{1}$$

where <…> denotes a time average (or a toroidal average) over the fast-scale turbulence, and f is any nonlinear function of the quantity Q. This problem has not yet received much attention. In the present note, we study how large the discrepancy is in Eq. (1) for a simple model problem of some practical importance.

The model problem chosen here is to calculate the condition for high-Z impurity avalanche due to self-sputtering of a high-Z wall, where the dominant nonlinearity is the temperature dependence of the ionization rate. The avalanche process requires that sputtered high-Z neutrals from the wall ionize and return to the wall to sputter more neutrals. Qualitatively, we know that impurity avalanche requires a sputtering yield Y greater than unity, which in turn requires energetic, high-Z ions. Low-Z materials have Y << 1, and even high-Z ions need energies in excess of several hundred eV to yield significant self-sputtering.[3] It has been inferred from previous experiments[4,5] that self-sputtering avalanche can occur in the vicinity of high-power ion cyclotron range of frequency (ICRF) antennas which contain high-Z components. Thus, this problem may be relevant to ITER (the International Thermonuclear Experimental Reactor)[6] which is considering the possibility of having ICRF antennas mounted near a high-Z first wall.[7]

The goal of the present calculation is not to obtain quantitative information, but to assess qualitatively whether (i) intermittency effects require a significant modification of

2

the usual transport code description, and (ii) whether blob- or ELM-induced self-sputtering of a high-Z wall is an issue that should be studied with more detailed and quantitative codes. In the rest of this note, we will use the term "blobs" to refer to the discrete plasma objects in the SOL with the understanding that the same physics applies to ELMs as well.

The one-dimensional (1D) model used here retains only variation in the radial direction, $x = R - R_{sep}$, and the trajectories $x(t)$ determine the location of the blob-neutral interactions. The SOL is assumed to extend from $x = 0$ (separatrix) to x_w (wall). The trajectories of the "world lines" and a schematic drawing of the model are given in Fig. 1. The blobs move from left to right, i.e. away from the last closed surface and towards the wall, with constant velocity v_{xb} (solid lines) and the sputtered neutrals move from right to left, i.e. away from the wall and towards the core plasma, with constant velocity v_{x0} (dashed lines). The number p of vertices in the SOL, i.e. intersection points between the blob and neutral world lines computed following a neutral pulse (black dots in Fig. 1), is given by

$$p = \left[\frac{x_w}{\tau_p v_*} \right]_{int} \quad , \quad \frac{1}{v_*} = \frac{1}{v_{x0}} + \frac{1}{v_{xb}} \quad . \tag{2}$$

Here, τ_p is the time between consecutive blobs, v_* is a hybrid ion-neutral velocity, and p is the largest integer bounded from above by $x_w / (v_* \tau_p)$. For the case sketched in Fig. 1, we see that $p = 2$.

Each blob interacts with the high-Z material in two ways. First, the blob creates a localized cloud or pulse of high-Z neutrals by (self) sputtering at the wall (this is discussed in more detail subsequently); second, other blobs collide with this neutral pulse (at the vertices shown in the figure) and partially ionize it. The plasma density in the blobs is assumed to be much larger than the background plasma, and effects of the background plasma are neglected. (Here, for simplicity we consider a single ionization

state, e.g. the first ionization state of each neutral atom.) The high-Z ions created in this way are assumed to be entrained by the internal electric field of the blob and to move back towards the wall with the same $\mathbf{E} \times \mathbf{B}$ velocity as the background plasma density. These entrained high-Z ions are the source of the self-sputtering computed in the model. Any high-Z neutral atoms not ionized in this initial collision continue to stream inwards towards the plasma and undergo additional ionization interactions with later blobs (at subsequent vertices shown in the figure). This results in a "ballistic" model, i.e. the ionization interaction is discrete in both space and time and depends on the trajectories of the blobs and neutral pulses.

Rather than treating a truly *intermittent* problem (in the sense of turbulence statistics), we use a *periodic* train of blobs to represent the discrete nature of the interactions in space and time. This is sufficient for present purposes. Each blob is modeled as a square pulse of radial width $2a_b$ and the blobs are spaced a distance $\Delta x_b = v_{xb}\,\tau_p$ apart, where τ_p is the period of the blob train. An important parameter characterizing the intermittency is the "packing fraction" $0 < \delta_b < 1$ of the blobs, defined here to be

$$\delta_b \equiv \frac{\bar{n}_e}{n_{eb}} = \frac{2a_b}{\Delta x_b} \quad , \tag{3}$$

where n_{eb} is the local electron density in the blob and $\bar{n}_e$ is the time-averaged density of the blob train. The resulting neutral pulses created by sputtering are also treated as a train of square pulses, each one initiated by the arrival of a blob at the wall.

For definiteness, let us consider a deuterium (D) plasma and a molybdenum (Mo) wall. The sputtering of D on Mo will not be very effective because of the atomic mass difference, but will provide a seed of high-Z Mo atoms that can in turn be ionized and produce sputtering by Mo ions impacting the Mo wall (i.e. "self-sputtering" of the wall material). The question to be answered by our model is whether the concentration of wall

4

atoms will grow, leading to a high-Z "*self-sputtering avalanche*", or decrease in time. We neglect the seeding process and formulate the model as an eigenvalue problem for the gain or growth factor per period, $g = e^{\gamma \tau_p}$, and the corresponding growth rate, $\gamma = \ln g / \tau_p$, where the blob train period τ_p is chosen as a typical waiting time between blob emissions. The avalanche condition is g > 1 or $\gamma > 0$. Referring again to Fig. 1, we note that the number of high-Z atoms (and ions) is multiplied by the factor g when the time is advanced by τ_p.

The sputtering and rf physics issues are characterized as follows. Let Y = Y(E) denote the Mo self-sputtering yield (number of sputtered atoms per incident ion) for an ion with energy E hitting the wall. As in previous work,[4] we use published data for the sputtering yield $Y_{90}(E)$ at 90 degree (normal) incidence.[8] In the far SOL, the ions flow along field lines which are almost tangent to the wall, so we multiply Y_{90} by a factor of 2, i.e. Y = 2 Y_{90}(E), to account for the larger sputtering yield at glancing incidence.[4]

For the ion energy, we choose E = 500 eV, which is a typical value for ions accelerated in rf sheath potentials. (A review of rf sheath physics can be found in Ref. 9.) The component of the rf field parallel to the equilibrium magnetic field **B** accelerates electrons out of the plasma, inducing a large rf sheath potential $\Phi_{rf} >> \Phi_{Bohm} \sim 3 T_e$ to confine the electrons and preserve ambipolarity. This sheath potential confines all but the most energetic electrons, and accelerates ions into the wall with high energy. Thus, the energy E is the rf sheath physics input to the present model, and reflects the fact that we are modeling the part of the high-Z wall which is in contact with field lines passing in front of a high-power ICRF antenna and having high sheath voltages at the contact points.

Ionization physics (only a single ionization state) is included in the model as follows. For simplicity, we neglect losses of heat and particle by transport along field lines, so that the blob density n_{eb} and temperature T_{eb} are assumed constant as the blob moves across the SOL. This approximation is valid in the limit of rapid cross-field

convection, $x_w / v_{xb} \ll \tau_{\|p}$ and $\tau_{\|E}$, where $\tau_{\|p} = L_\| / c_s$ and $\tau_{\|E}$ are the parallel particle and electron energy confinement times, and is sufficient for illustrating the physics of interest here. This assumption implies that the fraction f of neutrals ionized during each blob-neutral pulse collision (i.e. at each vertex in the model) is constant, and this permits simple analytic formulas. The generalization to a numerical code including parallel losses is straightforward but unenlightening. The ionization fraction f (defined such that $0 < f < 1$) can be taken as a constant input parameter to the model, or it can be expressed in terms of more basic parameters as

$$f = 1 - e^{-v_i \tau_i} \quad , \quad \tau_i = \frac{2a_b}{v_{x0} + v_{xb}} \quad , \tag{4}$$

where $v_i = n_e < \sigma v >_i$ is the ionization rate and τ_i is the interaction time between a neutral atom and a blob (in the rest frame of the neutral atom). We use a published formula and atomic physics data[10] to compute the ionization cross-section for the first ionization state of Mo.

The equations for our discrete model are given as follows. In Fig. 1, the variables N_j and Z_j denote the number of high-Z neutral atoms and ions, respectively, at the jth vertex. Unless otherwise noted, we henceforth omit the qualifier "high-Z" because it is understood that the model only tracks the wall atoms and ions. We follow the evolution of the ballistic interaction between the ions and neutrals starting with a reference vertex where Z_1/g ions hit the wall and generate N_0 neutrals. The equation for the number of neutrals sputtered at the wall (j = 1) by the ions in this blob is

$$N_0 = \frac{YZ_1}{g} \quad . \tag{5}$$

At interior vertices in the SOL , there are two conditions on the ions and neutrals. For j = 1, 2, ... p - 1, the number of neutrals free-streaming through the jth vertex is diminished by ionization of the neutral pulse:

$$N_j = (1-f)N_{j-1} \quad .$$

(6)

For j = 2, 3… p - 1, the number of ions (Z_j / g) already entrained in the blob and passing through the (j -1) vertex are enhanced by ionization of the neutral pulse from the previous (j – 2) vertex:

$$Z_j = g(Z_{j-1} - f\, N_{j-2}) \quad .$$

(7)

At the last vertex in the SOL (j = p), we assume no pass-through of high-Z ions from the core into the SOL, so that Z_p is due entirely to ionization of SOL neutrals:

$$Z_p = f\, N_{p-1}$$

(8)

We complete the system of equation by choosing the normalization

$$N_0 = 1 \quad .$$

(9)

This set of equations yields a geometric series which can be summed to give the following analytic dispersion relation for the growth factor g:

$$\frac{g^p - (1-f)^p}{f+g-1} = \frac{g^p}{f\, Y} \quad ,$$

(10)

where the ionization fraction f, sputtering yield Y and number of vertices p are assumed to be given. The growth rate of the sputtered neutrals (normalized to blob train period) is then given by

$$\gamma\, \tau_p = \ln g \quad .$$

(11)

It is useful to solve this dispersion relation analytically in limiting cases. First, we note that the factor $(1-f)^p$ can be neglected in two limits: (i) $f \rightarrow 1$ (strong ionization), and (ii) $p \rightarrow \infty$ for fixed f (closely packed blobs). In both cases we obtain $g = 1 + f(Y-1)$, implying that the high-Z impurity avalanche condition (g > 1) requires $Y > 1$. If $f(Y-1) << 1$, the growth rate for this case is given by $\gamma\, \tau_p \approx f(Y-1)$. In the limit $p \rightarrow 1$, where infrequent blob production is described by a single vertex model, one

obtains $g = f Y$ and avalanche requires $Y > 1/f$, which is much harder to satisfy. Thus, the physics in this model problem depends on the number of interactions (vertices) and thus on the discreteness of the transport.

We have also examined the correspondence between the growth rate calculated from our discrete interaction model in the limit $p \to \infty$ and the value of γ obtained in the continuum limit by solving the following fluid equations

$$\frac{\partial n_0}{\partial t} - v_{x0} \frac{\partial n_0}{\partial x} = -\nu_i n_0 \quad , \tag{12}$$

$$\frac{\partial n_z}{\partial t} + v_{xb} \frac{\partial n_z}{\partial x} = \nu_i n_0 \quad , \tag{13}$$

for the density n_0 of high-Z neutral atoms and n_z of high-Z ions subject to two boundary conditions: $n_0 v_{x0} = Y n_z v_{xb}$ (self-sputtering relation) at the wall ($x = x_w$) and $n_z = 0$ (no high-Z ions inside the confined plasma) at the last closed flux surface ($x = 0$). The dispersion relation of this continuum model has the form

$$\frac{Y\hat{v}}{(\hat{\gamma}+\hat{v})}\left[1 - e^{-(\hat{\gamma}+\hat{v})}\right] = 1 \tag{14}$$

where $\hat{\gamma} \equiv \gamma x_w / v_*$, $\hat{v} \equiv \nu_i x_w / v_{x0}$ and $\nu_i = n_e <\sigma v>_i$.

To make the desired correspondence, we consider the discrete model in the limit where there is a large number of small interactions. Thus, we let $f = f_1/p$ and $\tau_p = \tau_{p1}/p$ and take the limit $p \to \infty$ with f_1 and τ_{p1} held fixed. In this limit Eq. (10) yields

$$\frac{e^{\gamma \tau_{p1}} - e^{-f_1}}{f_1 + \gamma \tau_{p1}} = \frac{e^{\gamma \tau_{p1}}}{f_1 Y} \quad , \tag{15}$$

Expanding Eq. (4) gives $f \approx \nu_i \tau_i$, which is small because $\tau_i \propto a_b \propto 1/p$ where fixed δ_b was assumed. Using the definitions given previously, one can rewrite this linearized result for f in the following form

8

$$f = \frac{\delta_b \nu_i \tau_p}{1 + v_{x0}/v_{xb}} \quad \Rightarrow \quad f_1 = \frac{\delta_b \nu_i \tau_{p1}}{1 + v_{x0}/v_{xb}} \quad . \tag{16}$$

Finally, after some algebra using Eq. (2), one can show that $\hat{\gamma} \equiv \gamma x_w / v_* = \gamma \tau_{p1}$ and $\hat{v} \equiv \nu_i x_w / v_{x0} = f_1 / \delta_b$. Substituting these results into Eq. (14) yields Eq. (15) in the limits $p \to \infty$ and $\delta_b \to 1$. Thus, the discrete model corresponds to the usual continuum (fluid) model in the limit where the number of vertices becomes large and the blobs are tightly packed. In this continuum limit, we find that $\hat{\gamma} = p \gamma \tau_p \to p(g-1)$. We are interested in investigating how the solution changes in the discrete limit $\delta_b \to 0$.

The analysis requires that we solve Eq. (10) numerically, with the sputtering yield Y and ionization fraction f evaluated for Mo using empirical sputtering[8] and ionization[10] models. We will illustrate the dependence of the high-Z species growth rate on both the discreteness (δ_b) and the blob electron temperature T_{eb}. In varying the discreteness, we hold the mean density $\overline{n}_e$ and temperature $\overline{T}_e$ fixed so that the local density and temperature of the blob (or ELM) scale with the relevant packing fraction:

$$n_{eb} = \frac{\overline{n}_e}{\delta_n} \equiv \frac{\overline{n}_e}{\delta_b} \quad , \quad T_{eb} = \frac{\overline{T}_e}{\delta_T} \quad . \tag{17}$$

These relations simply express the fact that the local blob density and temperature exceed the mean values (in time or space) when the transport is discrete or intermittent. There is a "spikiness" to the density and temperature profiles, as typically observed on probes in the far SOL. This relation is clear for the density. In the case of the temperature, the argument is less clear. If we imagine that the SOL is filled with a cold, low-density plasma, then the concept of an average temperature makes sense, and in the discrete limit we expect that $\delta_T \ll 1$. For simplicity, we set $\delta_T = \delta_n \equiv \delta_b$ in the numerical work, where δ_b is defined in Eq. (3). Here, the assumption of strong convective cross-field transport, $x_w / v_{xb} \ll \tau_{\|E}$, is crucial to the assertion of temperature discreteness.

For the numerical work, we use the following parameters: $\bar{n}_e = 5 \times 10^{11}$ cm^{-3} (average SOL density); x_w = 8 cm (SOL width), a_b = 1 cm (blob radius); $v_{xb} = 10^5$ cm/s 10 (blob velocity); $v_{x0} = 10^5$ cm/s 10 (Mo neutral velocity), which corresponds to a sputtered neutral temperature of 1 eV; and E = 500 eV (kinetic energy of Mo ions impacting the wall). Including the factor of 2 enhancement of Y for glancing angle impact (discussed previously), we find Y $\approx$ 2 Y_{90}(E) = 1.8 for Mo. The local ionization fraction in the blob, $f(n_{eb}, T_{eb})$, is computed from Eqs. (4) and (17) holding $\bar{n}_e$ and $\bar{T}_e$ fixed. As we vary the packing fraction δ_b, the number of vertices in the SOL is given by [see Eqs. (2) and (3)]

$$ p = \left[\frac{x_w}{2 a_b} \frac{v_{xb}}{v_*} \delta_b \right]_{int} \equiv \left[\frac{\delta_b}{\delta_{crit}} \right]_{int}, \tag{18} $$

and scales as $p \propto \delta_b$; it follows that there are no blob - neutral pulse interactions in the SOL (i.e. $p < 1$) below a critical value, $\delta_b < \delta_{crit} = [(2 a_b / x_w)(v_* / v_{xb})]_{int}$.

Figure 2(a) shows how the ionization fraction varies with the intermittency parameter for two values of the average temperature, $\bar{T}_e$ = 1 and 10 eV; Fig. 2(b) shows the variation in the normalized growth rate $\hat{\gamma} \equiv \gamma x_w / v_*$ of high-Z (Mo) impurities in the SOL. The maximum variation among the curves occurs as $\delta_b \to 1$, for which the bottom curve ($\bar{T}_e \ll E_{ion}$) has negligible ionization (f = 0) and is thus stable to impurity avalanche. (Here, E_{ion} denotes the ionization energy, which is about 7 eV for the lowest ionization state of Mo.) The other curve has $\bar{T}_e \sim E_{ion}$ so that the ionization fraction is substantial, even in the limit $\delta_b \to 1$, and is unstable to avalanche ($\hat{\gamma} > 0$). In both cases, as the discreteness increases ($\delta_b \to 0$) at fixed average density and temperature, the *local* blob density and temperature increase, and hence the ionization fraction f increases, as shown in Fig. 2(a). Eventually, at small packing fraction even the low temperature curve goes unstable to avalanche in this 1D model, as shown in Fig. 2(b) (but see the discussion below of 2D effects). Heuristically, this effect is described by $f \sim \delta_b v_{i,eff}$,

where the effective ionization rate is defined as $\nu_{i,eff}(\overline{n}_e, \overline{T}_e) = \nu_i(\overline{n}_e/\delta_b, \overline{T}_e/\delta_b)$. Using an approximate ionization model, and taking the time average defined in Eq. (1), gives the scaling $f \sim \langle n_e \rangle \exp(-\delta_b E_{ion}/\langle T_e \rangle) \neq \langle n_e \exp(-E_{ion}/T_e) \rangle$.

In Fig. 2(b), we compare the discrete and continuum solutions and illustrate the behavior of the discrete solution as a function of blob packing fraction. The continuum solution for the two temperatures is given by Eq. (14) and is indicated in Fig. 2(b) by the two red dots. Note that the limit $\delta_b \rightarrow 1$ of the discrete model does not exactly coincide with the continuum solution, especially for the higher temperature case. Using Eq. (18) one can show that the number of vertices is $p \approx 7$ at $\delta_b = 1$ for the parameters used here, and thus does not satisfy the other condition ($p \rightarrow \infty$) for the continuum limit. As an exercise, we have verified that choosing the (untypical) value $a_b = 0.1$ cm yields $p = 79$ at $\delta_b = 1$ and gives excellent agreement between the discrete and continuum results.

We note that there are two competing effects determining $\hat{\gamma}$. First, the sawtooth pattern in growth rate in Fig. 2(b) is due to the addition of another blob-neutral pulse ionization event ($n \rightarrow n+1$) as δ_b increases, which tends to increase the growth rate. On the other hand, Eq. (17) implies that n_{eb} and T_{eb} decrease as δ_b increases (when the average values $\overline{n}_e$ and $\overline{T}_e$ are held constant), which reduces the growth rate. This figure shows that the the former effect dominates at high $\overline{T}_e$ and the latter effect wins at low $\overline{T}_e$.

The main point of our paper is perhaps best illustrated by Fig. 2(b), which shows that the discrete (low δ_b) and continuum limits ($\delta_b = 1$) are quite different. In the continuum case, the $\overline{T}_e = 1$ eV case is stable and the $\overline{T}_e = 10$ eV is unstable with a large growth rate. In the opposite limit, $\delta_{crit} \leq \delta_b \ll 1$, the system is unstable to sputtering avalanche (but with relatively small growth rates) for both temperatures. Finally, the possibility of avalanche disappears when $p < 1$ and $\delta_b < \delta_{crit}$, implying that the neutral pulse can stream across the SOL without encountering any blobs to ionize it. (This occurs in the region to the left of the dashed vertical line in Fig. 2b.) Thus, depending on the plasma and turbulence parameters, the discreteness effects can either greatly enhance or

reduce the possibility of impurity avalanche as compared with the continuum model. This illustrates the difficulty in doing these estimates with a transport code.

In conclusion, using a simple 1D ballistic model, we have investigated a typical nonlinear interaction of discrete particle and energy transport by blobs (or ELMs) with the first wall. We studied the effect of the ionization nonlinearity on the self-sputtering avalanche of the wall, assuming (i) a high-Z wall material, and (ii) large rf sheath potentials caused by ICRF heating. This problem illustrates both the complicated interaction of intermittent transport with nonlinearities [see Eq. (1)] and the fact that nonlinear rf effects (such as sheath formation) can interact in potentially important ways with edge turbulence. This is a largely unexplored subject.

The most important specific result of this calculation is the dispersion relation in Eq. (10), which shows analytically that the avalanche condition depends on the discreteness of the transport. This conclusion suggests that discrete (blobby or ELMy) intermittent transport should be included in realistic 2D impurity codes, especially in doing assessments of ITER, although it is not yet clear how to incorporate such effects in general within a 2D slow-time-scale framework.

When our 1D model is evaluated for a molybdenum wall, the numerical results indicate that high-Z avalanche can occur for reasonable parameters when steady transport is replaced by a small number of infrequent but very large plasma objects hitting the wall. This may be particularly important when the SOL transport is caused by ELMs (e.g. see the fast camera imaging results in Ref. 11). However, the present model cannot be used to make quantitative predictions because of a number of omitted effects, including both parallel transport and 2D effects. A 2D model is essential because consecutive blobs can be created at different poloidal locations, introducing an additional discreteness in the poloidal direction. This will reduce the number of effective blob-neutral interactions, implying an even greater role for the type of discreteness effects considered here.

Acknowledgements

Figure Captions

Fig. 1 (Color online) Sketch of the world lines in the SOL for the plasma blobs (red dashed lines) and the sputtered high-Z neutral pulses (green solid lines). The left boundary is the last closed surface, and the right boundary is the high-Z wall. Ionization interactions between blobs and neutral pulses for one sample line-segment occur at the black dots and the sputtering interaction is indicated by a cross. As time elapses, the growth in number of high-Z ions (Z_j) and high-Z neutrals (N_j) per period is denoted by the factor g, which is the eigenvalue of the dispersion relation derived in the text. The case shown has two ionization interactions in the SOL $(p = 2)$.

Fig. 2 (Color online) (a) the ionization fraction f and (b) the normalized growth rate $\hat{\gamma} \equiv \gamma x_w / v_*$ of high-Z (Mo) impurities in the SOL vs the blob packing fraction δ_b for two values of the average blob temperature, $\overline{T}_e = 1$ eV (solid black line) and 10 eV (dashed blue line). In (b) the horizontal line indicates the marginal stability point ($\hat{\gamma} = 0$) and the vertical dashed line indicates the value of δ_{crit} (no ionization occurs for $\delta_b < \delta_{crit}$). The two red dots indicate the solution of the continuum model equation, Eq. (14), for the two temperatures.
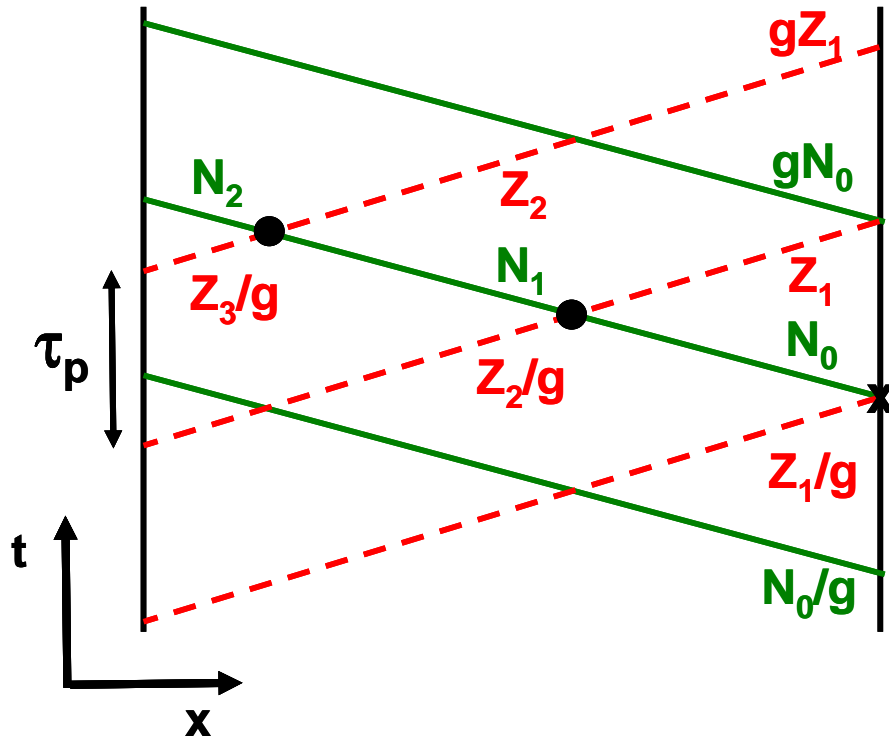
Fig. 1 (Color online) Sketch of the world lines in the SOL for the plasma blobs (red dashed lines) and the sputtered high-Z neutral pulses (green solid lines). The left boundary is the last closed surface, and the right boundary is the high-Z wall. Ionization interactions between blobs and neutral pulses for one sample line-segment occur at the black dots and the sputtering interaction is indicated by a cross. As time elapses, the growth in number of high-Z ions (Z_j) and high-Z neutrals (N_j) per period is denoted by the factor g, which is the eigenvalue of the dispersion relation derived in the text. The case shown has two ionization interactions ($p = 2$) in the SOL.
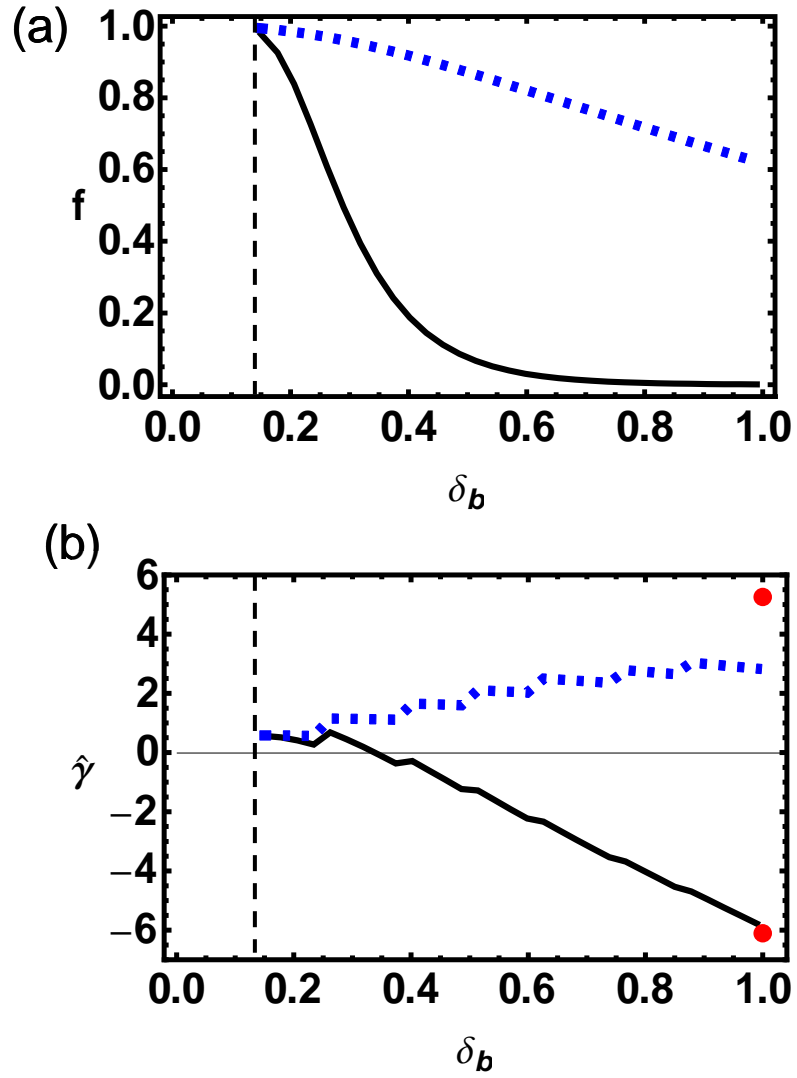
Fig. 2 (Color online) (a) the ionization fraction f and (b) the normalized growth rate $\hat{\gamma} \equiv \gamma x_w / v_*$ of high-Z (Mo) impurities in the SOL vs the blob packing fraction δ_b for two values of the average blob temperature, $\overline{T}_e = 1$ eV (solid black line) and 10 eV (dashed blue line). In (b) the horizontal line indicates the marginal stability point ($\hat{\gamma} = 0$) and the vertical dashed line indicates the value of δ_{crit} (no ionization occurs for $\delta_b < \delta_{crit}$). The two red dots indicate the solution of the continuum model equation, Eq. (14), for the two temperatures.

16

References

[1] S. J. Zweben, J.A. Boedo, O. Grulke, C. Hidalgo, B. LaBombard, R.J. Maqueda, P. Scarin, and J. L. Terry, Plasma Phys. Control. Fusion **49**, S1 (2007).

[2] S. I. Krasheninnikov, D. A. D'Ippolito and J. R. Myra, J. Plasma Phys. **74** (2008).

[3] J. Bohdansky, in *Data Compendium for Plasma-Surface Interactions*, Nucl. Fusion Special Issue 1984.

[4] D. A. D'Ippolito, J. R. Myra, M. Bures, and J. Jacquinot, Plasma Phys. Controlled Fusion **33**, 607 (1991).

[5] M. Bures et al., Plasma Phys. and Controlled Fusion **33**, 937 (1991).

[6] Progress in ITER Physics Basis Editors, Nucl. Fusion **47**, S1 (2007).

[7] B. Lipschultz, X. Bonnin, G. Counsell, A. Kallenbach, A. Kukushkin, K. Krieger, A. Leonard6, A. Loarte, et al., Nucl. Fusion **47** 1189, (2007).

[8] We use an analytic expression for the sputtering yield at normal incidence, Eq. (6.16) of Ref. 3, with empirical coefficents chosen to match the sputtering data [see Table 6.1 of Ref. 3].

[9] J. R. Myra, D. A. D'Ippolito, D. A. Russell, L. A. Berry, E. F. Jaeger, and M. D. Carter, Nucl. Fusion **46**, S455-S468 (2006).

[10] We use an analytic expression for the ionization rate coefficient, Eq. (4.3.25) of H. R. Griem and R. H. Lovberg, *Methods of Experimental Physics: Plasma Physics (Part A)*, vol. 9, (Academic Press, New York, 1970).

[11] J. H. Yu, J. A. Boedo, E. M. Hollmann, R. A. Moyer, D. L. Rudakov, and P. B. Snyder, Phys. Plasmas **15**, 032504 (2008).